

# Effective third-order susceptibility of silicon-nanocrystal-doped silica

Ivan D. Rukhlenko,<sup>1,\*</sup> Weiren Zhu,<sup>1</sup> Malin Premaratne,<sup>1</sup>  
and Govind P. Agrawal<sup>2</sup>

<sup>1</sup>Advanced Computing and Simulation Laboratory (A $\chi$ L), Department of Electrical and Computer Systems Engineering, Monash University, Clayton, VIC 3800, Australia

<sup>2</sup>The Institute of Optics, University of Rochester, Rochester, NY 14627, USA

\*[ivan.rukhlenko@monash.edu](mailto:ivan.rukhlenko@monash.edu)

**Abstract:** We derive approximate analytic expressions for the effective susceptibility tensor of a nonlinear composite, consisting of silicon nanocrystals embedded in fused silica. Two types of composites are considered: by assuming that (i) the crystallographic axes of different crystallites are the same, or (ii) crystallites are oriented randomly. In the first case, the tensor properties of the effective third-order susceptibility are shown to coincide with those of the bulk silicon. In the second case, however, the tensor properties of the susceptibility of the composite material are found to be quite different due to drastic modification of light interaction with optical phonons inside the composite. The newly derived expressions should be useful for modeling nonlinear optical phenomena in silica fibers and waveguides doped with silicon nanocrystals.

© 2012 Optical Society of America

**OCIS codes:** (999.9999) Silicon nanocrystals; (160.4330) Nonlinear optical materials; (190.4400) Nonlinear optics, materials; (260.2065) Effective medium theory; (190.0190) Nonlinear optics.

---

## References and links

1. R. Soref and J. Lorenzo, "All-silicon active and passive guided-wave components for  $\lambda = 1.3$  and  $1.6 \mu\text{m}$ ," IEEE J. Quantum Electron. **22**, 873–879 (1986).
2. J. Leuthold, C. Koos, and W. Freude, "Nonlinear silicon photonics," Nat. Photonics **4**, 535–544 (2010).
3. L. Pavesi and D. Lockwood, eds., *Silicon Photonics*, vol. 94 of *Topics in Applied Physics* (Springer-Verlag, Berlin, 2004).
4. D. Liang and J. E. Bowers, "Recent progress in lasers on silicon," Nat. Photonics **4**, 511–517 (2010).
5. I. D. Rukhlenko, C. Dissanayake, M. Premaratne, and G. P. Agrawal, "Maximization of net optical gain in silicon-waveguide Raman amplifiers," Opt. Express **17**, 5807–5814 (2009).
6. A. Martinez, J. Blasco, P. Sanchis, J. V. Galan, J. Garcia-Ruperez, E. Jordana, P. Gautier, Y. Lebour, S. Hernandez, R. Spano, R. Guider, N. Daldosso, B. Garrido, J. M. Fedeli, L. Pavesi, and J. Marti, "Ultrafast all-optical switching in a silicon-nanocrystal-based silicon slot waveguide at telecom wavelengths," Nano Lett. **10**, 1506–1511 (2010).
7. I. D. Rukhlenko, M. Premaratne, and G. P. Agrawal, "Analytical study of optical bistability in silicon-waveguide resonators," Opt. Express **17**, 22124–22137 (2009).
8. M. Paniccia, "Integrating silicon photonics," Nat. Photonics **4**, 498–499 (2010).
9. L. Pavesi and R. Turan, eds., *Silicon Nanocrystals: Fundamentals, Synthesis and Applications* (WILEY-VCH Verlag GmbH & Co. KGaA, Weinheim, 2010).
10. L. Khriachtchev, ed., *Silicon Nanophotonics: Basic Principles, Present Status and Perspectives* (Pan Stanford, Singapore, 2009).
11. I. D. Rukhlenko and M. Premaratne, "Optimization of nonlinear performance of silicon-nanocrystal cylindrical nanowires," IEEE Photon. J. **4**, 952–959 (2012).

12. F. D. Leonhardt and V. M. N. Passaro, "Dispersion engineered silicon nanocrystal slot waveguides for soliton ultrafast optical processing," *Adv. Optoelectron.* **2011**, 751498 (2011).
13. P. Sanchis, J. Blasco, A. Martínez, and J. Martí, "Design of silicon-based slot waveguide configurations for optimum nonlinear performance," *J. Lightwave Technol.* **25**, 1298–1305 (2007).
14. V. A. Belyakov, V. A. Burdov, R. Lockwood, and A. Meldrum, "Silicon nanocrystals: Fundamental theory and implications for stimulated emission," *Adv. Opt. Technol.* **2008**, 279502 (2008).
15. I. D. Rukhlenko, M. Premaratne, and G. P. Agrawal, "Effective mode area and its optimization in silicon-nanocrystal waveguides," *Opt. Lett.* **37**, 2295–2297 (2012).
16. D. Stroud and P. M. Hui, "Nonlinear susceptibilities of granular matter," *Phys. Rev. B* **37**, 8719–8724 (1988).
17. X. C. Zeng, D. J. Bergman, P. M. Hui, and D. Stroud, "Effective-medium theory for weakly nonlinear composites," *Phys. Rev. B* **38**, 10970–10973 (1988).
18. D. J. Bergman, "The dielectric constant of a composite material – a problem in classical physics," *Phys. Rep.* **43**, 377–407 (1978).
19. S. N. Volkov, J. J. Saarinen, and J. E. Sipe, "Effective medium theory for 2D disordered structures: A comparison to numerical simulations," *J. Mod. Opt.* **59**, 954–961 (2012).
20. W. Cai and V. Shalaev, *Optical Metamaterials: Fundamentals and Applications* (Springer, New York, 2010).
21. R. W. Boyd, R. J. Gehr, G. L. Fischer, and J. E. Sipe, "Nonlinear optical properties of nanocomposite materials," *Pure Appl. Opt.* **5**, 505–512 (1996).
22. J. D. Jackson, *Classical Electrodynamics*, 3rd ed. (Wiley, New York, 1998).
23. P. M. Hui, P. Cheung, and D. Stroud, "Theory of third harmonic generation in random composites of nonlinear dielectrics," *J. Appl. Phys.* **84**, 3451–3458 (1998).
24. D. Stroud, "Generalized effective-medium approach to the conductivity of an inhomogeneous material," *Phys. Rev. B* **12**, 3368–3373 (1975).
25. J. Sipe and R. Boyd, "Nanocomposite materials for nonlinear optics based on local field effects," in "Optical Properties of Nanostructured Random Media," vol. 82 of *Topics Appl. Phys.*, V. M. Shalaev, ed. (Springer-Verlag, Berlin Heidelberg, 2002), pp. 1–19.
26. G. L. Fischer, R. W. Boyd, R. J. Gehr, S. A. Jenekhe, J. A. Osaheni, J. E. Sipe, and L. A. Weller-Brophy, "Enhanced nonlinear optical response of composite materials," *Phys. Rev. Lett.* **74**, 1871–1874 (1995).
27. R. W. Boyd, *Nonlinear Optics*, 3rd ed. (Academic Press, San Diego, 2008).
28. J. Wei, A. Wirth, M. C. Downer, and B. S. Mendoza, "Second-harmonic and linear optical spectroscopic study of silicon nanocrystals embedded in SiO<sub>2</sub>," *Phys. Rev. B* **84**, 165316 (2011).
29. Y. Jiang, P. T. Wilson, M. C. Downer, C. W. White, and S. P. Withrow, "Second-harmonic generation from silicon nanocrystals embedded in SiO<sub>2</sub>," *Appl. Phys. Lett.* **78**, 766 (2001).
30. W. L. Mochan, J. A. Maytorena, B. S. Mendoza, and V. L. Brudny, "Second-harmonic generation in arrays of spherical particles," *Phys. Rev. B* **68**, 085318 (2003).
31. J. I. Dadap, J. Shan, K. B. Eisenthal, and T. F. Heinz, "Second-harmonic Rayleigh scattering from a sphere of centrosymmetric material," *Phys. Rev. Lett.* **83**, 4045–4048 (1999).
32. Q. Lin, O. J. Painter, and G. P. Agrawal, "Nonlinear optical phenomena in silicon waveguides: Modeling and applications," *Opt. Express* **15**, 16604–16644 (2007).
33. M. Premaratne and G. P. Agrawal, *Light Propagation in Gain Media* (Cambridge Univ. Press, Cambridge, 2011).
34. G. P. Agrawal, *Nonlinear Fiber Optics* (Academic Press, San Diego, 2007).
35. R. M. Murray, Z. Li, and S. S. Sastry, *A Mathematical Introduction to Robotic Manipulation* (CRC Press, Boca Raton, FL, 1994).
36. W. Grieshaber, E. Belorizky, and M. L. Berre, "A general method for tensor averaging and an application to polycrystalline materials," *Solid State Commun.* **93**, 805–809 (1995).
37. I. D. Rukhlenko, M. Premaratne, C. Dissanayake, and G. P. Agrawal, "Continuous-wave Raman amplification in silicon waveguides: Beyond the undepleted pump approximation," *Opt. Lett.* **34**, 536–538 (2009).
38. L. Yin, J. Zhang, P. M. Fauchet, and G. P. Agrawal, "Optical switching using nonlinear polarization rotation inside silicon waveguides," *Opt. Lett.* **34**, 476–478 (2009).
39. I. D. Rukhlenko, I. L. Garanovich, M. Premaratne, A. A. Sukhorukov, G. P. Agrawal, and Y. S. Kivshar, "Polarization rotation in silicon waveguides: Analytical modeling and applications," *IEEE Photon. J.* **2**, 423–435 (2010).
40. C. Torres-Torres, A. López-Suárez, R. Torres-Martínez, A. Rodríguez, J. A. Reyes-Esqueda, L. Castaneda, J. C. Alonso, and A. Oliver, "Modulation of the propagation speed of mechanical waves in silicon quantum dots embedded in a silicon-nitride film," *Opt. Express* **20**, 4784–4789 (2012).

---

## 1. Introduction

Even though silicon was recognized as an important material for photonics technology more than 25 years ago [1], the relevant theoretical concepts have begun to be put into practice only recently [2, 3]. A number of breakthroughs in the field of silicon photonics have made

possible the development of a variety of functional nonlinear devices, with both active and passive silicon elements. These devices not only can generate and amplify optical signals [4, 5] but can also modulate and switch them—either all-optically or electro-optically—at speeds approaching hundreds of gigabits per second [6, 7]. The realization of such ultrafast silicon photonic devices brings us closer to the moment when they will be combined with the microelectronics technology to build high-performance, low-cost, photonic integrated circuits [8].

A crucial step towards the development of silicon photonics was the discovery of unique optical properties of low-dimensional silicon [9, 10]. In particular, it was found that the ultrafast Kerr effect in silicon nanocrystals (Si NCs) may be, respectively, 10000 and 100 times stronger than that in fused silica (SiO<sub>2</sub>) and bulk silicon. Much like silicon-on-insulator waveguides, silica glass doped with Si NCs (Si-NCs/SiO<sub>2</sub> composite) enables tight confinement of optical fields, while its refractive index may be tuned to any value between 1.45 and 2.2 by simply changing the density of the Si NCs [11–13]. Furthermore, the optical response of Si NCs has a pronounced dependence on their size, thus providing a flexibility in the engineering of their nonlinear properties. These and other features guarantee that Si NCs can serve silicon photonics by improving the performance of optical memories, wavelength converters, and modulators, as well as by enabling power-efficient amplifiers and light sources [14].

Numerical modeling of light propagation through Si-NC-doped silica waveguides requires a knowledge of the effective optical parameters of the Si-NCs/SiO<sub>2</sub> composite [11, 15]. The reason is that it is impracticable to study the nonlinear effects in Si NCs by solving Maxwell equations for the whole composite while treating each NC individually. To do so, one would have to consider more than 100 000 nanocrystals per micrometer of waveguide with a 0.01- $\mu\text{m}^2$  cross section, in which Si NCs of 2.5 nm diameter have a volume fraction as small as 10%. It is evident that it would be extremely challenging to solve numerically such a nonlinear problem.

To enable theoretical studies of the nonlinear optical phenomena in a Si-NCs/SiO<sub>2</sub> composite, we relate its effective susceptibility to the third-order susceptibility tensor of silicon and linear permittivities of the composite's constituents. We begin by considering the situation in which all nanocrystals have the same orientation with respect to the macroscopic sample of the composite. In our derivation we closely follow the effective-medium approach to the calculation of the nonlinear susceptibilities of granular matter [16]. It was initially applied by Zeng *et al.* [17] to random composites featuring a weakly nonlinear relation between electric field and electric displacement of the form  $\mathbf{D} = (\epsilon + \chi|\mathbf{E}|^2)\mathbf{E}$ , where  $\chi$  is a scalar. Our derivation shows that the values of all components of the effective susceptibility tensor are reduced (with respect to those in silicon) by the same factor that depends on the volume fraction of Si NCs. We then extend our analysis and calculate the effective susceptibility for a situation in which NCs are randomly orientated in space with a uniform distribution. In this case, the anisotropy of the nonlinear optical response of the whole composite is different from that of bulk silicon. In particular, the Raman response resulting from the vibrational subsystem of the NCs is modified the most.

## 2. Identically oriented nanocrystals

### 2.1. Linear effective permittivity of Si-NCs/SiO<sub>2</sub> composite

The response of both Si NCs and fused silica to a weak optical field is essentially linear and isotropic. In this instance, the space-averaged electric displacement  $\mathcal{D}_k$  ( $k = x, y, z$ ) and space-averaged electric field

$$\mathcal{E}_k = \frac{1}{V} \int E_k(\mathbf{r}) dV \quad (1)$$

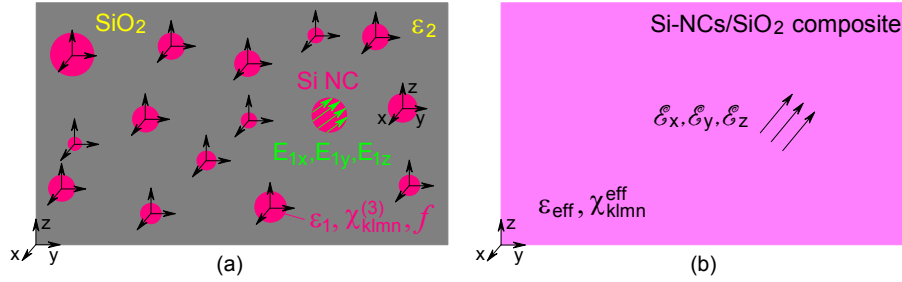


Fig. 1. (a) Identically oriented Si NCs embedded in a SiO<sub>2</sub> matrix of permittivity  $\epsilon_2$ . Nanocrystals are characterized by permittivity  $\epsilon_1$ , nonlinear susceptibility tensor  $\chi_{klmn}^{(3)}$ , and volume filling factor  $f$ ; electric field  $(E_{1x}, E_{1y}, E_{1z})$  inside Si NCs is assumed to be uniform. (b) Homogeneous Si-NCs/SiO<sub>2</sub> composite and the space-averaged electric field  $(\mathcal{E}_x, \mathcal{E}_y, \mathcal{E}_z)$  inside it; the composite is characterized by the effective parameters  $\epsilon_{\text{eff}}$  and  $\chi_{klmn}^{\text{eff}}$ .

inside the Si-NCs/SiO<sub>2</sub> composite are related simply through the linear effective permittivity  $\epsilon_{\text{eff}}$  as  $\mathcal{D}_k = \epsilon_{\text{eff}} \mathcal{E}_k$ . If the local electric field  $\mathbf{E}(\mathbf{r}) = (E_x, E_y, E_z)$  is known everywhere inside the composite, then the linear effective permittivity may be calculated using the definition [18]

$$\epsilon_{\text{eff}} = \frac{1}{V} \int \epsilon(\mathbf{r}) \left( \frac{\mathbf{E}(\mathbf{r})}{\mathcal{E}} \right)^2 dV, \quad (2)$$

where  $\mathcal{E}^2 = \mathcal{E}_x^2 + \mathcal{E}_y^2 + \mathcal{E}_z^2$  and the integration is evaluated over the entire volume  $V$  of the composite. The space-dependent permittivity  $\epsilon(\mathbf{r}) = \epsilon_1 \vartheta_1(\mathbf{r}) + \epsilon_2 \vartheta_2(\mathbf{r})$  is expressed here through the permittivity  $\epsilon_1$  of silicon and permittivity  $\epsilon_2$  of silica, as well as through  $\vartheta$  functions defined as

$$\vartheta_j(\mathbf{r}) = \begin{cases} 1 & \text{when } \mathbf{r} \text{ is inside the } j\text{th medium;} \\ 0 & \text{otherwise.} \end{cases} \quad (3)$$

Since no analytical expression generally exists for the local field, one often resorts to the mean-field approach in order to calculate  $\epsilon_{\text{eff}}$  [19, 20]. Specifically, for the Si-NCs/SiO<sub>2</sub> composite with the volume fraction  $f$  of the NCs, the effective-medium theory gives

$$\epsilon_{\text{eff}}(\epsilon_1, \epsilon_2, f) = \frac{1}{4} \left[ u + (u^2 + 8\epsilon_1\epsilon_2)^{1/2} \right], \quad (4)$$

where  $u = (3f - 1)\epsilon_1 + (2 - 3f)\epsilon_2$ . This equation assumes that Si NCs are spherical in shape and their mean size is much smaller than the optical wavelength; this assumption is valid for most practical situations of interest [6, 10].

## 2.2. Third-order effective susceptibility of Si-NCs/SiO<sub>2</sub> composite

To simplify the following calculation, we neglect the third-order susceptibility  $\chi^{(3)}$  of silica completely in the following calculation. This assumption is justified in practice because  $\chi^{(3)}$  for silicon NCs is much larger than that for silica and is valid as long as the filling factor of Si NCs exceeds, respectively, 0.001% and 0.1% when Raman scattering and Kerr effect are considered. We also assume the average NC diameter to be larger than the exciton Bohr radius in bulk silicon (which is about 5 nm) and neglect the effect of quantum confinement on the third-order susceptibility of silicon. With these simplifications, we can define the effective

susceptibility tensor of a Si-NCs/SiO<sub>2</sub> composite in a way similar to Eq. (2) [16, 17]:

$$\chi_{klmn}^{\text{eff}} = \frac{1}{V_1} \int \chi_{klmn}^{(3)}(\mathbf{r}) \frac{E_k(\mathbf{r})E_l(\mathbf{r})E_m^*(\mathbf{r})E_n(\mathbf{r})}{\mathcal{E}^4} dV_1,$$

where  $\chi_{klmn}^{(3)}(\mathbf{r})$  is the third-order susceptibility of silicon (which may be a function of coordinates if the crystallographic axes of different nanocrystals do not coincide) and the integration is over the nanocrystals' volume  $V_1 = fV$ . Without knowing the exact field distribution inside Si NCs, however, it is more practical to introduce this susceptibility using averaged fields and displacements,

$$\mathcal{D}_k = \varepsilon_{\text{eff}} \mathcal{E}_k + \sum_{lmn} \chi_{klmn}^{\text{eff}} \mathcal{E}_l \mathcal{E}_m^* \mathcal{E}_n, \quad (5)$$

and resort to the effective-medium theory [21]. If we assume that the crystallographic axes  $x$ ,  $y$ , and  $z$  of all Si NCs have the same spatial orientation, as in Fig. 1(a), then the components of the electric displacement inside the nanocrystals is given by the expression

$$D_{1k} = \varepsilon_1 E_{1k} + \sum_{lmn} \chi_{klmn}^{(3)} E_{1l} E_{1m}^* E_{1n} \equiv \hat{\varepsilon}_1 E_{1k}, \quad (6)$$

where the nonlinear permittivity  $\hat{\varepsilon}_1$  of Si NCs is implicitly defined. Now  $\chi_{klmn}^{\text{eff}}$  may be expressed through  $\chi_{klmn}^{(3)}$  by invoking an approximate relation

$$\mathcal{D}_k \approx \varepsilon_{\text{eff}}(\hat{\varepsilon}_1, \varepsilon_2, f) \mathcal{E}_k, \quad (7)$$

which is valid provided the nonlinear terms in Eqs. (5) and (6) are small compared to the linear ones [17].

Expanding the function  $\varepsilon_{\text{eff}}(\hat{\varepsilon}_1, \varepsilon_2, f)$  in Taylor series about the linear permittivity of silicon, yields

$$\begin{aligned} \mathcal{D}_k &\approx \varepsilon_{\text{eff}}(\varepsilon_1, \varepsilon_2, f) \mathcal{E}_k + \frac{\partial \varepsilon_{\text{eff}}(\hat{\varepsilon}_1, \varepsilon_2, f)}{\partial \hat{\varepsilon}_1} (\hat{\varepsilon}_1 - \varepsilon_1) \mathcal{E}_k \\ &= \varepsilon_{\text{eff}} \mathcal{E}_k + \frac{\partial \varepsilon_{\text{eff}}}{\partial \varepsilon_1} \frac{\mathcal{E}_k}{E_{1k}} \sum_{lmn} \chi_{klmn}^{(3)} E_{1l} E_{1m}^* E_{1n}. \end{aligned} \quad (8)$$

The local field  $E_{1k}$  may be related to the averaged field  $\mathcal{E}_k$  using an auxiliary effective permittivity  $\varepsilon_{\text{aux}}$ , which satisfies the relation

$$\varepsilon_{\text{aux}} \int E_k(\mathbf{r}) dV = \int \varepsilon(\mathbf{r}) E_k(\mathbf{r}) dV.$$

By differentiating both sides of this relation with respect to  $\varepsilon_1$ , we obtain

$$\mathcal{E}_k \frac{\partial \varepsilon_{\text{aux}}}{\partial \varepsilon_1} = \frac{1}{V} \int \vartheta_1(\mathbf{r}) E_k(\mathbf{r}) dV = f \langle E_{1k} \rangle, \quad (9)$$

where the angle brackets denote averaging over the volume of Si NCs. In a similar fashion, Eq. (2) gives

$$\frac{\partial \varepsilon_{\text{eff}}}{\partial \varepsilon_1} = f \frac{\langle \mathbf{E}_1^2 \rangle}{\mathcal{E}^2} \approx f \frac{\langle \mathbf{E}_1 \rangle^2}{\mathcal{E}^2} = \frac{1}{f} \left( \frac{\partial \varepsilon_{\text{aux}}}{\partial \varepsilon_1} \right)^2. \quad (10)$$

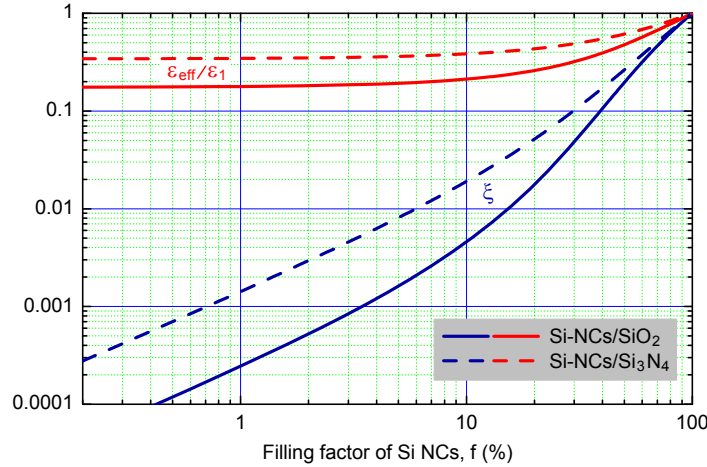


Fig. 2. Ratios  $\epsilon_{\text{eff}}/\epsilon_1$  and  $\xi$  are plotted as a function of filling factor  $f$  for Si-NCs/SiO<sub>2</sub> (solid curves) and Si-NCs/Si<sub>3</sub>N<sub>4</sub> (dashed curves) composites using  $\epsilon_1 = 12$  with  $\epsilon_2 = 2.1$  for SiO<sub>2</sub> and  $\epsilon_2 = 4.1$  for Si<sub>3</sub>N<sub>4</sub>.

In deriving this result, we have assumed that electric field is almost uniform inside the nanocrystals, i.e.,  $E_{1k} \approx \langle E_{1k} \rangle$ . With this assumption and Eqs. (8) to (10), we obtain

$$\mathcal{D}_k \approx \epsilon_{\text{eff}} \mathcal{E}_k + \frac{1}{f} \frac{\partial \epsilon_{\text{eff}}}{\partial \epsilon_1} \left| \frac{\partial \epsilon_{\text{eff}}}{\partial \epsilon_1} \right| \sum_{lmn} \chi_{klmn}^{(3)} \mathcal{E}_l \mathcal{E}_m^* \mathcal{E}_n.$$

The comparison of this equality with Eq. (5) shows that

$$\chi_{klmn}^{\text{eff}} = \frac{1}{f} \frac{\partial \epsilon_{\text{eff}}}{\partial \epsilon_1} \left| \frac{\partial \epsilon_{\text{eff}}}{\partial \epsilon_1} \right| \chi_{klmn}^{(3)}. \quad (11)$$

The effective susceptibility tensor is thus obtained via a multiplication of  $\chi_{klmn}^{(3)}$  by the scalar attenuation factor, which according to Eq. (4) is given by

$$\xi = \frac{[(3f - 1)\epsilon_{\text{eff}} + \epsilon_2]^2}{f(u^2 + 8\epsilon_1\epsilon_2)}.$$

This result is valid to the first order in  $\chi_{klmn}^{(3)}$ . Since electric field is constant inside a dielectric sphere placed in an initially uniform electric field [22], Eq. (11) becomes more accurate for weakly interacting Si NCs, i.e., for a sample with a smaller filling factor. In the case of a larger filling factor, an accurate relation between the third-order susceptibility of silicon and that of Si-NCs/SiO<sub>2</sub> composite may be obtained numerically within the framework of the generalized effective-medium approach developed by Stroud [23, 24].

The effective permittivity and attenuation factor of the Si-NCs/SiO<sub>2</sub> composite are plotted in Fig. 2 as solid curves. It is seen that the components of the effective susceptibility tensor are about 200 times smaller for a Si-NCs/SiO<sub>2</sub> composite than those of Si NCs for moderate filling factors of about 10%. However, thanks to the strong optical nonlinearities of Si NCs, these may still be comparable to, and even exceed, the nonlinear coefficients in bulk silicon. For example, the Kerr coefficient  $n_2$  at a wavelength of 1.55  $\mu\text{m}$  is approximately equal to  $4 \times 10^{-14} \text{ cm}^2/\text{W}$  for bulk silicon and to  $2.5 \times 10^{-14} \text{ cm}^2/\text{W}$  for the Si-NCs/SiO<sub>2</sub> composite in which Si NCs with  $n_2 = 2 \times 10^{-12} \text{ cm}^2/\text{W}$  occupy 17% of the volume [6]. The value of  $n_2^{\text{eff}}$  may be increased

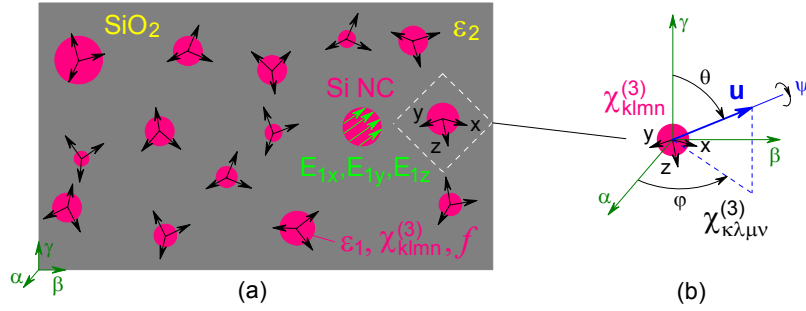


Fig. 3. (a) Randomly oriented Si NCs embedded in SiO<sub>2</sub> matrix. Orientation of each nanocrystal, with respect to the Cartesian axes  $\alpha$ ,  $\beta$ , and  $\gamma$ , is characterized by the respective directions of its crystallographic axes  $x$ ,  $y$ , and  $z$ . (b) Rotation by an angle  $\psi \in [0, 2\pi)$  around a unit vector  $\mathbf{u}$  (set by angles  $\vartheta$  and  $\varphi$ ) brings crystallographic axes of Si NC into coincidence with the axes  $\alpha$ ,  $\beta$ , and  $\gamma$ .

by using a host medium with higher permittivity [25, 26]. For instance, if Si<sub>3</sub>N<sub>4</sub> with  $\epsilon_2 = 4.1$  is used instead of SiO<sub>2</sub> in the above example, we obtain  $n_2^{\text{eff}} \approx 8.1 \times 10^{-14} \text{ cm}^2/\text{W}$ . For  $f \ll 1$ , the attenuation factor for Si-NCs/SiO<sub>2</sub> may be approximated as  $\xi \approx 81f/(2 + \epsilon_1/\epsilon_2)^4 \approx 0.22f$  [20, 27].

It is interesting to note that Si-NCs/SiO<sub>2</sub> composite may exhibit dipolar second-harmonic (SH) due to the effect of NC interfaces, despite the fact that bulk silicon is a centrosymmetric medium and can generate SH only through the quadrupolar nonlinearity [28, 29]. The theories of SH generation by a single centrosymmetric NC and a disordered composite of such NCs were developed in Refs. [30, 31].

It is also worth noting that Eq. (11) naturally generalizes the result of Zeng *et al.* [17] to the case of identically oriented crystallites possessing a tensorial third-order susceptibility.

### 3. Randomly oriented nanocrystals

Consider now the situation where the crystallographic axes of different Si NCs have all possible orientations in space, as is shown schematically in Fig. 3(a). The effective nonlinear susceptibility in this case is still defined by Eq. (5), but the constitutive relation in Eq. (6) is no longer valid for an arbitrary nanocrystal. As a result of this, each component of the effective susceptibility tensor becomes dependent on several components of  $\chi_{klmn}^{(3)}$ , and its calculation requires a knowledge of the exact tensorial form of the nonlinear optical susceptibility of silicon.

#### 3.1. Nonlinear optical susceptibility of silicon

The third-order susceptibility of silicon may be represented as a sum of contributions from bound electrons and optical phonons [32]

$$\chi_{klmn}^{(3)}(\omega; \omega_1, \omega_2, \omega_3) = \chi_{xxxx}^e(\omega) \mathcal{K}_{klmn} + \frac{1}{2} [H(\omega_1 + \omega_2) \mathcal{R}_{klmn} + H(\omega_2 + \omega_3) \mathcal{R}_{knml}], \quad (12)$$

where  $\chi_{xxxx}^e(\omega)$  is a complex constant,  $H(\omega)$  is the Raman gain profile,

$$\mathcal{K}_{klmn} = (\rho/3) (\delta_{kl} \delta_{mn} + \delta_{km} \delta_{ln} + \delta_{kn} \delta_{lm}) + (1 - \rho) \delta_{kl} \delta_{lm} \delta_{mn}, \quad (13a)$$

$$\mathcal{R}_{klmn} = \delta_{km} \delta_{ln} + \delta_{kn} \delta_{lm} - 2\delta_{kl} \delta_{lm} \delta_{mn}, \quad (13b)$$

$\rho = 3\chi_{xxyy}^e/\chi_{xxxx}^e$  is the anisotropy factor, and  $\delta_{ij}$  is the Kronecker delta. The first term in Eq. (12) leads to the Kerr effect and two-photon absorption, and the remaining terms lead

to stimulated Raman scattering [33, 34]. It is important to keep in mind that these effects not only exhibit different tensorial properties but are also characterized by significantly different response times.

### 3.2. Susceptibility tensor averaging

Suppose that the crystallographic axes  $\{x, y, z\}$  of a certain sub-ensemble of the entire Si-NC ensemble may be brought in to coincide with the reference frame  $\{\alpha, \beta, \gamma\}$  of the macroscopic sample via their rotation by angles from  $\psi$  to  $\psi + d\psi$  around radius vectors lying within the infinitesimal solid angle  $d\Omega = \sin \vartheta d\vartheta d\varphi$  about the unit vector  $\mathbf{u}$ , whose position in the reference frame is determined by polar angle  $\vartheta$  and azimuth  $\varphi$  [see Fig. 3(b)]. Then the transformed susceptibility tensor characterizing the sub-ensemble can be written as

$$\chi_{\kappa\lambda\mu\nu}^{(3)} = \sum_{klmn} R_{\kappa k} R_{\lambda l} R_{\mu m} R_{\nu n} \chi_{klmn}^{(3)}, \quad (14)$$

where the rotation matrix is given by the Rodrigues' formula [35]

$$R(\vartheta, \varphi, \psi) = \begin{pmatrix} \cos \psi & -\cos \vartheta \sin \psi & \sin \varphi \sin \vartheta \sin \psi \\ \cos \vartheta \sin \psi & \cos \psi & -\cos \varphi \sin \vartheta \sin \psi \\ -\sin \varphi \sin \vartheta \sin \psi & \cos \varphi \sin \vartheta \sin \psi & \cos \psi \end{pmatrix} + (1 - \cos \psi) \begin{pmatrix} \cos^2 \varphi \sin^2 \vartheta & \cos \varphi \sin \varphi \sin^2 \vartheta & \cos \varphi \cos \vartheta \sin \vartheta \\ \cos \varphi \sin \varphi \sin^2 \vartheta & \sin^2 \varphi \sin^2 \vartheta & \sin \varphi \cos \vartheta \sin \vartheta \\ \cos \varphi \cos \vartheta \sin \vartheta & \sin \varphi \cos \vartheta \sin \vartheta & \cos^2 \vartheta \end{pmatrix}. \quad (15)$$

As discussed in Section 2.2, the contribution of the sub-ensemble of almost identically oriented Si NCs to the effective third-order susceptibility of the Si-NCs/SiO<sub>2</sub> composite is given by the expression

$$\chi_{\kappa\lambda\mu\nu}^{\text{eff}} = \frac{1}{f} \frac{\partial \varepsilon_{\text{eff}}}{\partial \varepsilon_1} \left| \frac{\partial \varepsilon_{\text{eff}}}{\partial \varepsilon_1} \right| \chi_{\kappa\lambda\mu\nu}^{(3)}.$$

Its averaging over a uniform distribution of nanocrystal orientations in space yields the effective susceptibility tensor of the entire composite,

$$\langle \chi_{\kappa\lambda\mu\nu}^{\text{eff}} \rangle = \frac{1}{8\pi^2} \int_0^\pi \sin \vartheta d\vartheta \int_0^{2\pi} d\varphi \int_0^{2\pi} d\psi \chi_{\kappa\lambda\mu\nu}^{\text{eff}}(\vartheta, \varphi, \psi). \quad (16)$$

This expression may be evaluated either directly [using Eqs. (14) and (15)] or using a general method based on finding the rotationally invariant part of the tensor in spherical coordinates [36].

Equations (14)–(16) show that the effective susceptibility tensor of the Si-NCs/SiO<sub>2</sub> composite that consists of randomly oriented nanocrystals may be conveniently split into electronic and Raman parts, as is done in Eq. (12). The tensor properties of each part can be found by averaging the respective tensors over the possible spacial orientations of the crystallites. This procedure may be simplified by noticing that tensors  $\delta_{kl}\delta_{mn}$ ,  $\delta_{km}\delta_{ln}$ , and  $\delta_{kn}\delta_{lm}$  are rotationally invariant. Applying the averaging procedure defined in Eq. (16) to the triple product in Eq. (13), we obtain

$$\langle \delta_{kl}\delta_{lm}\delta_{mn} \rangle = \frac{8}{45} (\delta_{kl}\delta_{mn} + \delta_{km}\delta_{ln} + \delta_{kn}\delta_{lm}) + \frac{1}{9} \delta_{kl}\delta_{lm}\delta_{mn}.$$

Using the preceding result in Eq. (16), the averaged value of  $\mathcal{H}_{\kappa\lambda\mu\nu}$  is found to be

$$\langle \mathcal{H}_{\kappa\lambda\mu\nu} \rangle = \frac{8+7\rho}{45} (\delta_{\kappa\lambda}\delta_{\mu\nu} + \delta_{\kappa\mu}\delta_{\lambda\nu} + \delta_{\kappa\nu}\delta_{\lambda\mu}) + \frac{1-\rho}{9} \delta_{\kappa\lambda}\delta_{\lambda\mu}\delta_{\mu\nu}. \quad (17)$$

Since the susceptibility tensor of an individual Si NC has only 21 nonzero components, this tensor also has only 21 nonzero components. The numerical factors for these components from Eq. (17) are found to be

$$\begin{aligned}\alpha\alpha\alpha\alpha &= \beta\beta\beta\beta = \gamma\gamma\gamma\gamma = \frac{29+16\rho}{45} \approx 1.1, \\ \alpha\alpha\beta\beta &= \alpha\beta\alpha\beta = \alpha\beta\beta\alpha = \dots = \frac{8+7\rho}{45} \approx 0.375,\end{aligned}$$

where we used  $\rho \approx 1.27$  near the 1.55- $\mu\text{m}$  wavelength [32]. It is seen that the averaging of the electronic part of the susceptibility tensor leads to about 10% increase in the values of diagonal components and 13% increase in the values of off-diagonal components.

A similar calculation can be performed for the Raman part of the third-order susceptibility. We find that  $\langle \mathcal{R}_{\kappa\lambda\mu\nu} \rangle$  is given by

$$\langle \mathcal{R}_{\kappa\lambda\mu\nu} \rangle = \frac{29}{45} (\delta_{\kappa\mu} \delta_{\lambda\nu} + \delta_{\kappa\nu} \delta_{\lambda\mu}) - \frac{16}{45} \delta_{\kappa\lambda} \delta_{\mu\nu} - \frac{2}{9} \delta_{\kappa\lambda} \delta_{\lambda\mu} \delta_{\mu\nu}. \quad (18)$$

We see that the averaging over NC orientations drastically modifies the interaction of an optical field with phonons in the Si-NCs/SiO<sub>2</sub> composite from that in individual nanocrystals. Even though the tensor  $\mathcal{R}_{\kappa\lambda\mu\nu}$  has only 12 nonzero components (equal to unity), the averaged tensor  $\langle \mathcal{R}_{\kappa\lambda\mu\nu} \rangle$  is characterized by 21 nonzero components. The components analogous to those of tensor  $\mathcal{R}_{klmn}$  have a value that is reduced considerably from 1:

$$\alpha\beta\alpha\beta = \alpha\beta\beta\alpha = \beta\gamma\beta\gamma = \dots = \frac{29}{45}.$$

However, this reduction leads to additional 9 components of the averaged tensor to become nonzero with values

$$\begin{aligned}\alpha\alpha\alpha\alpha &= \beta\beta\beta\beta = \gamma\gamma\gamma\gamma = \frac{32}{45}, \\ \alpha\alpha\beta\beta &= \alpha\alpha\gamma\gamma = \gamma\gamma\beta\beta = \dots = -\frac{16}{45}.\end{aligned}$$

These results imply that the dynamics of Raman amplification in a Si-NCs/SiO<sub>2</sub> composite will be different from that in a silicon-on-insulator waveguide [37]. It simply follows from the fact that, unlike the crystallographic axes of individual nanocrystals, the reference axes associated with the composite as a whole can be chosen arbitrarily. One consequence of this feature is that stimulated Raman scattering occurs in Si-NCs/SiO<sub>2</sub> composites regardless of the polarizations of pump and signal waves.

From a practical viewpoint, it is important to note that the averaging of the third-order susceptibility over the orientations of Si NCs does not make the nonlinear response of the Si-NCs/SiO<sub>2</sub> composite isotropic. This feature makes fused silica doped with randomly oriented Si NCs an attractive medium for polarization-sensitive applications, such as optical switching [38] or power equalization [39], that utilize nonlinear polarization rotation through cross-phase modulation. This statement does not apply to such nonlinear phenomena as thermo-optic effect [7] and electrostriction [40], which are essentially isotropic in individual Si NCs. Since such effects are often related to free carriers generated through two-photon absorption, they develop on nanosecond time scales and may cause the nonlinear response of the composite to vary with pulse width.

We emphasize that our theory is only applicable to those nonlinearities of silicon that can be described by the third-order susceptibility tensor; it does not include such effects as free-carrier absorption, which is essentially a fifth-order effect [32].

#### 4. Conclusions

We have derived approximate analytic expressions for the effective third-order susceptibility of Si-NCs/SiO<sub>2</sub> composites consisting of nanocrystals with either identically or randomly oriented crystallographic axes. We showed that when the orientations of the crystallographic axes in different crystallites are the same, the effective susceptibility of the composite may be simply obtained via a multiplication of the susceptibility tensor of silicon by a constant factor. On the other hand, if the crystallites are oriented in space randomly, then the effective susceptibility has tensor properties which are significantly different from those of silicon susceptibility. In the case of the Kerr nonlinearity, the values are enhanced by 10% or more depending on the susceptibility component.

Much more dramatic changes occur in the case of Raman susceptibility due to a modification of the interaction between the optical field and phonons inside the composite. In particular, some components that vanish in bulk silicon or planar silicon waveguides acquire a finite value in the case of Si-NCs/SiO<sub>2</sub> composites. The new form of Raman susceptibility has practical consequences if Si NCs are used to make Raman amplifiers and lasers in place of silicon planar waveguides. Results obtained in this paper should be useful for modeling nonlinear propagation through Si-NCs/SiO<sub>2</sub> fibers, which are promising candidates for realization of all-optical functions on a photonic chip.

#### Acknowledgments

This work is sponsored by the Australian Research Council, through its Discovery Early Career Researcher Award DE120100055. The work of W. Zhu and M. Premaratne is supported by the Australian Research Council through its Discovery Grant scheme under grant DP110100713.